

Single-dot spectroscopy of boron and phosphorus codoped silicon quantum dots

Takashi Kanno, Hiroshi Sugimoto, Anna Fucikova, Jan Valenta, and Minoru Fujii

Citation: *Journal of Applied Physics* **120**, 164307 (2016); doi: 10.1063/1.4965986

View online: <http://dx.doi.org/10.1063/1.4965986>

View Table of Contents: <http://scitation.aip.org/content/aip/journal/jap/120/16?ver=pdfcov>

Published by the [AIP Publishing](#)

Articles you may be interested in

[Photoluminescence study of high density Si quantum dots with Ge core](#)

J. Appl. Phys. **119**, 033103 (2016); 10.1063/1.4940348

[Silicon nanocrystals with high boron and phosphorus concentration hydrophilic shell—Raman scattering and X-ray photoelectron spectroscopic studies](#)

J. Appl. Phys. **115**, 084301 (2014); 10.1063/1.4866497

[Localization effects in the tunnel barriers of phosphorus-doped silicon quantum dots](#)

AIP Advances **2**, 022114 (2012); 10.1063/1.4707165

[Effect of surface passivation on dopant distribution in Si quantum dots: The case of B and P doping](#)

Appl. Phys. Lett. **98**, 173103 (2011); 10.1063/1.3583663

[Effects of boron and phosphorus doping on the photoluminescence of self-assembled germanium quantum dots](#)

Appl. Phys. Lett. **94**, 183103 (2009); 10.1063/1.3114377

Single-dot spectroscopy of boron and phosphorus codoped silicon quantum dots

Takashi Kanno,¹ Hiroshi Sugimoto,¹ Anna Fucikova,² Jan Valenta,² and Minoru Fujii^{1,a)}

¹*Department of Electrical and Electronic Engineering, Graduate School of Engineering, Kobe University, Rokkodai, Nada, Kobe 657-8501, Japan*

²*Department of Chemical Physics and Optics, Faculty of Mathematics and Physics, Charles University, Ke Karlovu 3, CZ-121 16 Prague 2, Czechia*

(Received 9 August 2016; accepted 10 October 2016; published online 27 October 2016)

Boron (B) and phosphorous (P) codoped silicon quantum dots (Si QDs) are dispersible in polar solvents without organic ligands, and exhibit size controllable photoluminescence (PL) from 0.85 to 1.85 eV due to the electronic transitions between the donor and the acceptor states. We study the PL spectra of the codoped Si QDs at room temperature and at 77 K. We show that the broad PL band of codoped colloidal Si QDs (full width at half maximum is over 400 meV) is composed of narrower PL bands of individual QDs with different PL energies. We also show that the PL linewidth of individual codoped Si QDs is almost twice as large as those of undoped Si QDs. In contrast to the significant narrowing of the PL linewidth of undoped Si QDs at low temperatures, that of codoped Si QDs is almost independent of the temperature except for a few very small QDs. These results suggest that a large number of B and P are doped in a QD and there are a number of non-identical luminescence centers in each QD. *Published by AIP Publishing.*

[<http://dx.doi.org/10.1063/1.4965986>]

I. INTRODUCTION

Bulk silicon (Si) crystal is not suitable for light emitting applications due to the indirect nature of the energy band structure. Since the observation of visible photoluminescence (PL) from porous Si,¹ Si quantum dots (QDs) have been actively studied as a promising material for optoelectronic devices^{2–5} as well as fluorescence markers in bioimaging and biosensing.^{6,7} The luminescence property of Si QDs can be controlled by the size,^{8,9} surface termination,^{10,11} chemical doping via surface organic molecules,¹² and substitutional impurity doping. Recently, the importance of the substitutional impurity doping to Si QDs has been recognized for the optoelectronic device applications, and the development of doped Si QDs has been reported.^{13–18} Furthermore, the preferential location of doped impurities and the energy state structures of doped Si QDs have been studied theoretically.^{19–24}

Impurity doping modifies not only the energy state structures of Si QDs but also the chemical properties. For example, simultaneously boron (B) and phosphorus (P) doped Si QDs are dispersible in polar solvents without organic surface ligands due to the negative surface potential induced by a heavily B and P codoped surface layer.^{25–27} Therefore, one can produce all-inorganic colloidal Si QDs by B and P codoping.^{25,28,29} Because of the high water dispersibility, bright near infrared (NIR) luminescence, high photo-stability, high pH stability, etc., the codoped Si QDs are a promising alternative to organic dyes for bioimaging and biosensing.³⁰ *In vitro* fluorescence imaging of cancer cells by codoped Si QDs has been recently demonstrated.³¹

The size-dependence of the energy state structure of B and P codoped Si QDs has been studied by PL spectroscopy,³² photoemission yield spectroscopy (PYS),³³ and valence band X-ray photoelectron spectroscopy (XPS).³³ These measurements reveal that the PL of codoped Si QDs arises from the transition between the donor to acceptor states in the bandgap, and the PL energy is several hundred meV lower than that of undoped Si QDs of a comparable size. The position of the Fermi level in the bandgap is also estimated; the Fermi level of codoped Si QDs is close to the valence band when the size is large, and it approaches the middle of the bandgap when the size is below ~ 3 nm.³³ The PL decay dynamics are also different from those of undoped Si QDs. The lifetime is shorter than those reported for undoped Si QDs, and the detection energy dependence is much smaller.³²

Although it has been previously demonstrated that impurity doping is an effective method to modify the optical response of Si QDs, quantitative understanding of the energy state structure, by comparing experimental data with theoretical calculations, has not been successful. The difficulty arises mainly from inhomogeneous broadening of the optical response of codoped Si QDs. In fact, the full width at half maximum (FWHM) of codoped Si QDs is much larger than that of undoped Si QDs.^{34,35} This is probably due to inhomogeneity of the impurity sites and numbers as well as the size and the shape. Different techniques have been developed to take away the inhomogeneity. Mastronardi *et al.* and Miller *et al.* succeeded in size purification of Si QDs using density gradient ultracentrifugation.^{36,37} This is a very powerful technique to remove inhomogeneous broadening by size distribution, but is not effective for the broadening arising from the distributions of impurity sites and numbers. Spectroscopic

^{a)}Electronic mail: fujii@eedept.kobe-u.ac.jp. Tel.: +81-78-803-6081.

TABLE I. List of samples.

Sample	RT				77 K				
	$d_{\text{ave}}^{\text{a}}$ (nm)	$E_{\text{ens}}^{\text{b}}$ (eV)	FWHM (meV)	$E_{\text{sin}}^{\text{c}}$ (eV)	FWHM (meV)	$E_{\text{ens}}^{\text{b}}$ (eV)	FWHM (meV)	$E_{\text{sin}}^{\text{c}}$ (eV)	FWHM (meV)
T1000	2.0	1.76	408	1.74 ± 0.05	240 ± 58	1.78	397	1.75 ± 0.05	269 ± 90
T1050	2.7	1.59	426	1.58 ± 0.06	240 ± 50	1.66	389	1.63 ± 0.03	244 ± 47
T1100	3.5	1.43	386	1.42 ± 0.04	224 ± 46	1.45	356	1.43 ± 0.05	239 ± 67

^a d_{ave} is the average QD diameter estimated by TEM observation.

^b E_{ens} is the PL peak energy of an ensemble of QDs.

^c E_{sin} is the average PL peak energy of single QDs and the standard deviation.

techniques such as hole burning spectroscopy,^{38,39} fluorescence line narrowing spectroscopy,^{40,41} and single-dot spectroscopy^{42,43} have been applied to study homogeneous linewidth of Si QDs. Among them, the most successful is the single-dot spectroscopy, which observes PL from a single QD on a low QD density substrate ($\sim 1 \text{ QD}/\mu\text{m}^2$) using a fluorescence microscope. FWHM of undoped Si QDs is reported to be 100–200 meV at room temperature.^{44–54} It reduces to 10–30 meV at 80 K (Refs. 47 and 55) and $\sim 200 \mu\text{eV}$ at 10 K.⁵⁶

In this work, we perform single-dot spectroscopy for B and P codoped Si QDs with different sizes. We show that the FWHMs of single codoped Si QDs are almost twice larger than those of undoped Si QDs at room temperature. We also show that narrowing of the width at low temperature (LT), which has been observed in undoped Si QDs, is not observed except in a few very small QDs.

II. EXPERIMENTAL

Colloidal B and P codoped Si QDs were prepared using the method used in our previous work.²⁵ Borophosphosilicate glass (BPSG) films containing B and P codoped Si QDs were first prepared by co-sputtering of Si, B_2O_3 , P_2O_5 , and SiO_2 and annealing at 1000, 1050, and 1100 °C for 30 min in a nitrogen atmosphere. The film was dissolved in a hydrofluoric acid (HF) solution for 1 h in order to etch out the BPSG matrices. The isolated Si QDs were separated from the HF solution by centrifugation and then transferred to methanol. A majority of Si QDs were dispersed in methanol. Precipitates were removed by centrifugation, and only the supernatant liquid was collected. Similarly, undoped Si QDs embedded in the SiO_2 matrix were fabricated by sputtering of Si and SiO_2 , and annealing at 1100 °C in the same manner. Unlike codoped Si QDs, undoped Si QDs form aggregates and precipitate in methanol. The list of the samples studied is shown in Table I. Hereafter, we refer to the samples by the name designated in the leftmost column of the table. The number in a sample name represents the annealing temperature.

Figure 1(a) shows a photograph of the colloidal solution of T1100. The solution remains clear and precipitates are not formed over several years. Figure 1(b) shows a high-resolution transmission electron microscope (TEM) (JEOL, JEM-2100F) image of Si QDs prepared by drop-casting the solution on a carbon-coated copper grid. Lattice fringe corresponding to {111} planes of Si crystal (0.314 nm) can be seen. In TEM image, no three-dimensional agglomerates

of Si QDs were observed due to the perfect dispersion in methanol. Figure 1(c) shows an atomic force microscope (AFM) (Park Systems, NX10) topography image of Si QDs on a fused quartz substrate. The QDs are isolated on the substrate. The size of the QDs estimated from the height profiles (Fig. 1(d)) is consistent with the size distribution obtained from TEM images. These results indicate that by simply drop-casting diluted solution, we can prepare samples for single-dot spectroscopy. The samples for single-dot spectroscopy were prepared by dropping 1.5 μl colloidal Si QDs ($\sim 1 \mu\text{g}/\text{ml}$) onto fused quartz substrates for room temperature measurements and onto Si substrates for low temperature measurements.

PL spectra of colloidal solutions were measured by a spectrophotometer (HORIBA, Fluorolog-3). The excitation source was a monochromatized xenon lamp (405 nm). PL images and spectra of single Si QDs were obtained by using an imaging spectrometer (Acton SP-2300i) equipped with a liquid nitrogen cooled charge coupled device (CCD) (Princeton Instruments, Spec-10:400B) connected to an inverted optical microscope

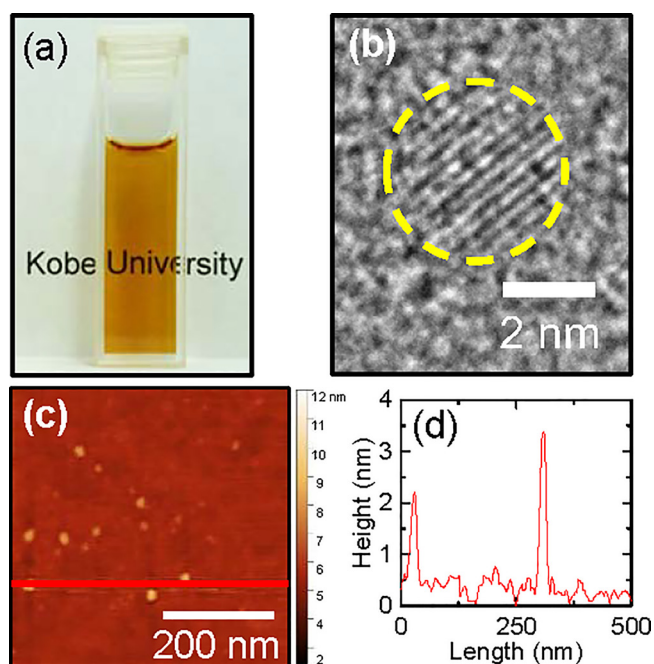


FIG. 1. (a) Photograph of colloidal codoped Si QDs in methanol (T1100). (b) High-resolution TEM image of a Si QD (T1100). (c) AFM topography image of Si QDs on a fused quartz substrate (T1050). (d) Height profile at the position marked in the topography image. The profile is obtained by subtracting the lowest height as an offset value from the measured height.

(Olympus IX-71, objective lens: $100\times/0.8$ at RT and $40\times/0.6$ at LT). The excitation source was a 405 nm semiconductor laser ($\sim 1\text{ W/cm}^2$ at sample). For low temperature measurements, samples were mounted on a liquid nitrogen flow cryostat (Janis, ST-500) and cooled down to 77 K. The sequence of the measurements is shown in the [supplementary material](#) (Figure S1). All spectra were corrected for the spectral response of the apparatus.

III. RESULTS AND DISCUSSION

Figure 2(a) shows the PL spectra of colloidal Si QDs in methanol. The size dependent shift of the PL can be clearly seen. The PL energy is several hundred meV lower than those of undoped Si QDs of comparable size,³² and the PL is considered to arise from electronic transitions between donor and acceptor states.³³ The FWHM of the PL bands is around 400 meV, which is much broader than those reported for

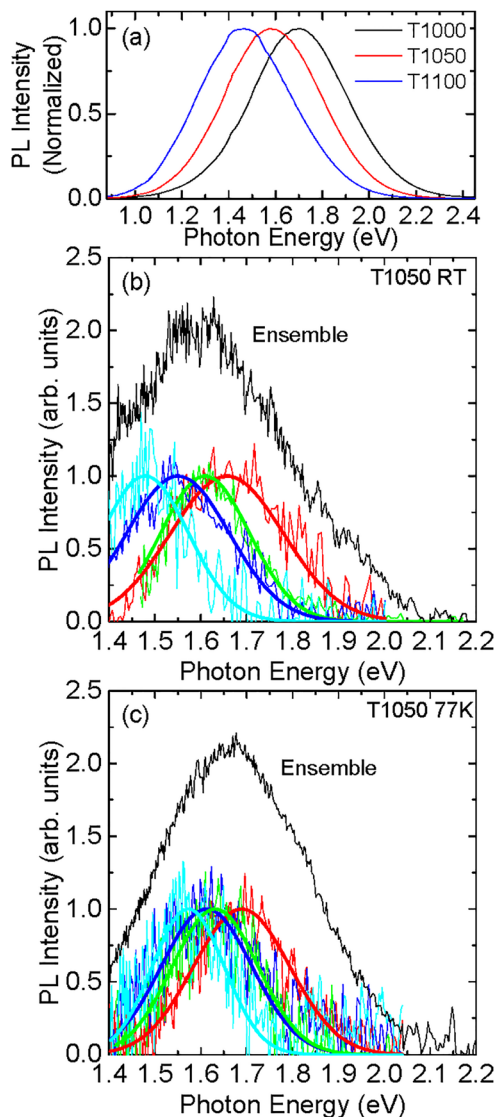


FIG. 2. (a) The PL spectra of colloidal Si QDs dispersed in methanol. ((b), (c)) Normalized PL spectra of single codoped Si QDs (T1050) measured at (b) room temperature and (c) 77 K. The spectra are fitted by a Gaussian function. The black solid lines are the PL spectra obtained from larger areas containing large numbers of Si QDs.

undoped Si QDs.^{34,35} In Fig. 2(b), the PL spectra of Si QDs on a quartz substrate at room temperature is shown (T1050). The spectrum labeled “ensemble” is obtained by detecting a large area, which contains about 100 Si QDs, while the others are those of single Si QDs. The spectra of single Si QDs are fitted by Gaussian functions. The PL peak energy (1.59 eV) and the FWHM (426 meV) of the “ensemble” are almost the same as those of the colloidal solution. This indicates that the PL property of codoped Si QDs is not strongly modified by drying in air (in contrast to some organically passivated QDs). The ensemble PL spectrum shifts to higher energy (1.66 eV) at 77 K. However, no significant change of the FWHM (389 meV) is observed.

The PL spectra of single Si QDs are much narrower than that of the ensemble; the PL FWHM is from 223 to 290 meV, nearly the half of that of the ensemble. The PL peak energy varies from QD to QD, although all the spectra are located within the broad PL band of the ensemble. Figure 2(c) shows the PL spectra of single codoped Si QDs and the ensemble at 77 K. Similar to the room temperature data, the FWHM of single Si QDs is much narrower than that of the ensemble. The PL spectra of other samples are shown in the [supplementary material](#) (Figures S2 and S3).

Figures 3(a)–3(c) show the histograms of PL peak energies of codoped Si QDs together with the PL spectra of the ensembles. The data are obtained for more than 50 single QDs. The distributions of the PL peak energies are in good agreement with the PL spectra of ensembles, indicating that the broad PL of the ensembles is due to the distribution of the PL peak energies of individual QDs. Figures 3(d)–3(f) are the data obtained at 77 K. There is a slight narrowing and a tiny blue-shift of the PL peak distributions.

Figure 4 shows the histograms of PL FWHMs of single codoped Si QDs. For all the samples, the FWHM is distributed in a wide range. At room temperature, the largest FWHM is around 350 meV and the smallest one is around 100 meV. The average FWHM is ~ 250 meV, which is larger than those

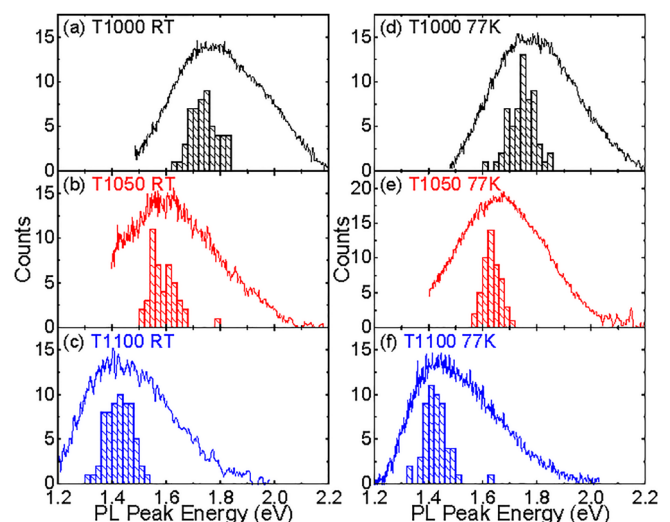


FIG. 3. Histograms of PL peak energy of codoped Si QDs measured at ((a)–(c)) room temperature and ((d)–(f)) 77 K. ((a), (d)) T1000, ((b), (e)) T1050, ((c), (f)) T1100. Solid lines are the PL spectra obtained from larger areas containing large number of Si QDs.

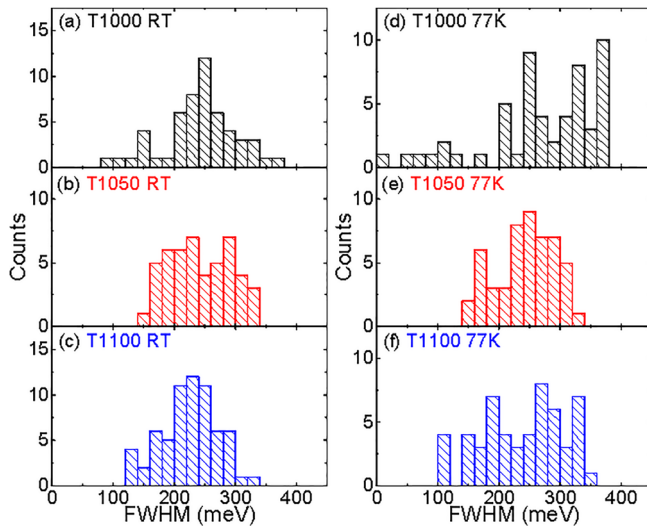


FIG. 4. Histograms of PL FWHM of codoped Si QDs measured at ((a)–(c)) room temperature and ((d)–(f)) 77 K. ((a), (d)) T1000, ((b), (e)) T1050, ((c), (f)) T1100.

reported for undoped Si QDs luminescing in the same energy range.^{45–47,50,53} For T1050 and T1100, no significant difference can be seen between room temperature and 77 K. On the other hand, in T1000, several QDs have the FWHM smaller than 100 meV at 77 K. This will be discussed later.

Figure 5(a) shows the relationship between the FWHM and the energy of the PL at room temperature. The data of undoped Si QDs obtained in this work and those taken from literature are also shown. The gray area represents the typical range of the FWHM of undoped Si QDs, which is 50–200 meV independent of the PL energy.^{46–54} On the other hand, the FWHM of B and P codoped Si QDs is distributed from 100 to 350 meV. The average FWHM is almost twice as large in codoped Si QDs as that in undoped Si QDs. In undoped Si QDs, the PL linewidth is considered to be determined by the coupling of the optical transitions with the momentum conservation phonons (TO phonon at the X point: 56 meV and at the Γ point: 64 meV).⁵⁷ In this model, the largest width was limited to ~ 130 meV, and thus, very large FWHM of codoped Si QDs can not be explained. One possible reason for the large width may be that there is more than one non-identical luminescence center in each QD due to the doping of large numbers of B and P atoms. In Ref. 32, the average number of B and P atoms per a Si QD is estimated. In the present samples, more than 10 B and P atoms are doped in each QD, and a number of them are considered to be doped in the substitutional sites.²⁶ Theoretical calculations demonstrate that the energy state structures of Si QDs depend strongly on the location of the impurity sites and the number.^{21,22,58,59} Therefore, doping of a large number of impurities and existence of a number of luminescent centers in a QD may result in a significant broadening of the PL band.

In Figure 5(a), a few QDs in T1000 have the FWHM comparable to those of undoped Si QDs. The average diameter of T1000 is 2 nm. At this size, one impurity atom corresponds to the doping concentration of $\sim 2.4 \times 10^{20} \text{ cm}^{-3}$, which is comparable to bulk solid solubility of P ($4 \times 10^{20} \text{ cm}^{-3}$). It is plausible that, in some QDs in T1000, there are no active

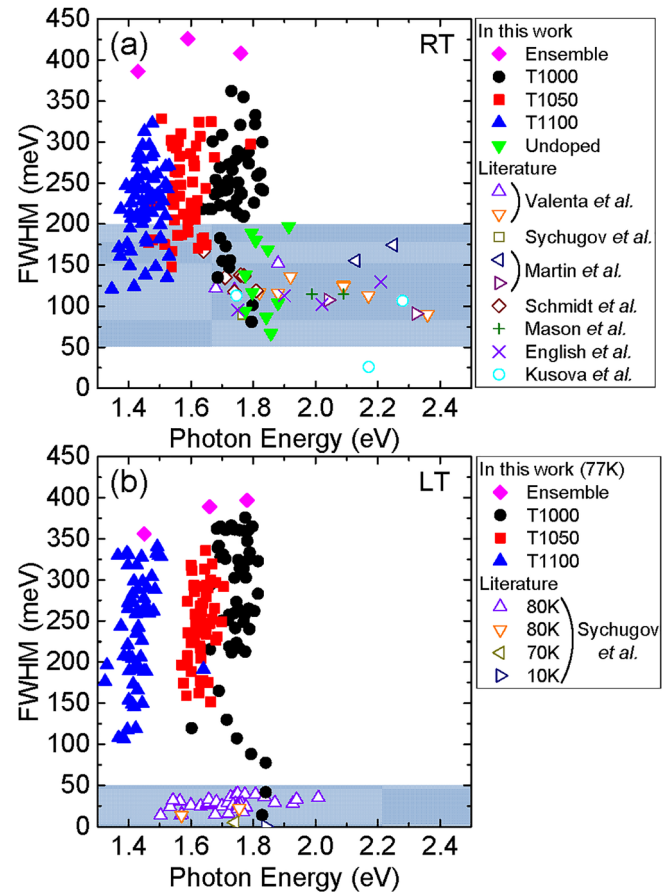


FIG. 5. Relation between the PL FWHM and the PL peak energy measured at (a) room temperature and (b) 77 K. Filled symbols represent experimental data in this work. Open symbols represent the data of undoped Si QDs obtained from Refs. 46–54 in (a) and Refs. 47, 55, 56, and 60 in (b).

impurities, which results in the PL spectra with the FWHM comparable to that of undoped ones.

Figure 5(b) shows the relationship between the FWHM and the PL peak energy at 77 K. As shown by the shadow, the FWHM of undoped Si QDs is smaller than 50 meV, which is much smaller than those at room temperature. On the other hand, the FWHM of the codoped Si QDs does not strongly depend on the temperature. This supports the model that the PL width of codoped Si QDs is determined by the distribution of the impurity sites in individual QDs.

Although the FWHM of almost all codoped Si QDs is insensitive to the measured temperature, there are a few exceptions in T1000. In Figure 5(b), several QDs have the FWHM smaller than 50 meV at 77 K, which is comparable to that of undoped Si QDs. In these QDs, impurities are considered to be absent. As discussed above, in Si QD ensembles, the PL peak energy of codoped QDs is smaller than that of undoped ones. If impurities are not doped in Si QDs with narrow PL bands, the PL energy should be higher than others with broad PL bands. Although we do not have enough number of narrow spectra for the statistical analyses, the PL energies of QDs with narrow bands are at almost the highest end of the distribution (Fig. 5(b)).

Figure 6 shows an example of the sharp PL. The width of the peak is about 15 meV. The peak seems to have a broad satellite at the low energy side of the main peak. Similar

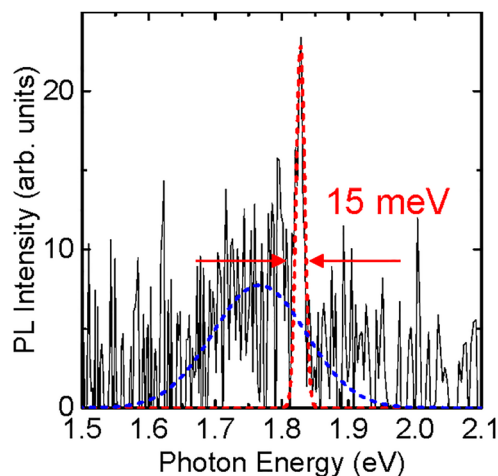


FIG. 6. A PL spectrum of a single Si QD (T1000) at 77 K. The spectrum is fitted by two Gaussian functions.

spectra have been observed in undoped Si QDs at low temperatures.⁵⁵ Usually, the narrow band is assigned to a zero-phonon transition and the low-energy one to a phonon-assisted transition with the emission of a momentum conservation TO phonon.^{55,60} Similar explanation might be applied to the spectrum in Fig. 6, although the low-energy band is much broader than those reported in undoped Si QDs. Another possible explanation of the broad satellite band is the overlap of PL spectra of one undoped and one codoped QDs.

IV. CONCLUSION

We have studied the PL spectra of B and P codoped Si QDs by single-dot spectroscopy. Similar to the case of undoped Si QDs, the very broad PL bands of codoped Si QDs observed for the colloidal solution and the ensemble were partly due to the wide variation of the PL peak energy between QDs. However, we also found that the PL width of individual codoped QDs was nearly twice larger than that of undoped Si QDs at room temperature. The large PL width of individual QDs may suggest that there are several luminescent centers in each QD, and the variation of the local environment of the impurity sites results in the broadening. The difference of the PL width between undoped and codoped Si QDs was enhanced at low temperatures. In undoped Si QDs, the width decreases significantly due to the lower probability of phonon absorption. On the other hand, in codoped Si QDs, the width is almost independent of the measured temperature except for a few very small QDs. The temperature insensitiveness supports the model that a number of non-identical luminescence centers exist in each QD. In a few very small QDs, a very sharp PL peak with a phonon satellite, similar to that reported for undoped Si QDs, is observed. In these QDs, impurities are expected to be absent.

SUPPLEMENTARY MATERIAL

See [supplementary material](#) for method of single-dot spectroscopy of single Si QDs and PL spectra from different single Si QDs.

ACKNOWLEDGMENTS

The authors thank Y. Fukuda and A. Otsuki for contributions to this work. This work was partly supported by the 2015 JST Visegrad Group (V4)-Japan Joint Research Project on Advanced Materials (MSMT Project No. 8F15001, cofinanced by the International Visegrad Fund) and JSPS KAKENHI Grant No. 16H03828. T.K. and H.S. acknowledge the support from Grant-in-Aid for JSPS Research Fellow (27-4138 and 26-3120).

- ¹L. T. Canham, *Appl. Phys. Lett.* **57**, 1046 (1990).
- ²C. Y. Liu, Z. C. Holman, and U. R. Kortshagen, *Nano Lett.* **9**, 449 (2009).
- ³Z. C. Holman, C. Y. Liu, and U. R. Kortshagen, *Nano Lett.* **10**, 2661 (2010).
- ⁴K. Y. Cheng, R. Anthony, U. R. Kortshagen, and R. J. Holmes, *Nano Lett.* **11**, 1952 (2011).
- ⁵F. Maier-Flaig, J. Rinck, M. Stephan, T. Bocksrocker, M. Bruns, C. Kübel, A. K. Powell, G. A. Ozin, and U. Lemmer, *Nano Lett.* **13**, 475 (2013).
- ⁶P. Das and N. R. Jana, *ACS Appl. Mater. Interfaces* **6**, 4301 (2014).
- ⁷F. Peng, Y. Su, Y. Zhong, C. Fan, S.-T. Lee, and Y. He, *Acc. Chem. Res.* **47**, 612 (2014).
- ⁸A. Gupta, M. T. Swihart, and H. Wiggers, *Adv. Funct. Mater.* **19**, 696 (2009).
- ⁹C. M. Hessel, D. Reid, M. G. Panthani, M. R. Rasch, B. W. Goodfellow, J. Wei, H. Fujii, V. Akhavan, and B. A. Korgel, *Chem. Mater.* **24**, 393 (2012).
- ¹⁰M. Dasog, G. B. De Los Reyes, L. V. Titova, F. A. Hegmann, and J. G. C. Veinot, *ACS Nano* **8**, 9636 (2014).
- ¹¹X. Cheng, R. Gondosiswanto, S. Ciampi, P. J. Reece, and J. J. Gooding, *Chem. Commun.* **48**, 11874 (2012).
- ¹²S. Mouri, Y. Miyauchi, and K. Matsuda, *Nano Lett.* **13**, 5944 (2013).
- ¹³X. D. Pi, R. Gresback, R. W. Liptak, S. A. Campbell, and U. Kortshagen, *Appl. Phys. Lett.* **92**, 123102 (2008).
- ¹⁴S. Zhou, X. Pi, Z. Ni, Y. Ding, Y. Jiang, C. Jin, C. Delerue, D. Yang, and T. Nozaki, *ACS Nano* **9**, 378 (2015).
- ¹⁵S. Zhou, Z. Ni, Y. Ding, M. Sugaya, X. Pi, and T. Nozaki, *ACS Photonics* **3**, 415 (2016).
- ¹⁶R. N. Pereira, A. R. Stegner, T. Andlauer, K. Klein, H. Wiggers, M. S. Brandt, and M. Stutzmann, *Phys. Rev. B* **79**, 161304 (2009).
- ¹⁷M. T. Björk, H. Schmid, J. Knoch, H. Riel, and W. Riess, *Nat. Nanotechnol.* **4**, 103 (2009).
- ¹⁸D. König, S. Gutsch, H. Gnaser, M. Wahl, M. Kopnarski, J. Göttlicher, R. Steininger, M. Zacharias, and D. Hiller, *Sci. Rep.* **5**, 9702 (2015).
- ¹⁹C. Delerue, M. Lannoo, G. Allan, and E. Martin, *Thin Solid Films* **255**, 27 (1995).
- ²⁰F. Iori and S. Ossicini, *Phys. E* **41**, 939 (2009).
- ²¹R. Guerra and S. Ossicini, *J. Am. Chem. Soc.* **136**, 4404 (2014).
- ²²X. Pi, X. Chen, and D. Yang, *J. Phys. Chem. C* **115**, 9838 (2011).
- ²³J. H. Eom, T. L. Chan, and J. R. Chelikowsky, *Solid State Commun.* **150**, 130 (2010).
- ²⁴T.-L. Chan, H. Kwak, J.-H. Eom, S. B. Zhang, and J. R. Chelikowsky, *Phys. Rev. B* **82**, 115421 (2010).
- ²⁵H. Sugimoto, M. Fujii, K. Imakita, S. Hayashi, and K. Akamatsu, *J. Phys. Chem. C* **116**, 17969 (2012).
- ²⁶M. Fujii, H. Sugimoto, M. Hasegawa, and K. Imakita, *J. Appl. Phys.* **115**, 084301 (2014).
- ²⁷K. Nomoto, H. Sugimoto, A. Breen, A. V. Ceguerra, T. Kanno, S. P. Ringer, I. P. Wurfl, G. J. Conibeer, and M. Fujii, *J. Phys. Chem. C* **120**, 17845 (2016).
- ²⁸M. Fukuda, M. Fujii, H. Sugimoto, K. Imakita, and S. Hayashi, *Opt. Lett.* **36**, 4026 (2011).
- ²⁹M. Fujii, H. Sugimoto, and K. Imakita, *Nanotechnology* **27**, 262001 (2016).
- ³⁰H. Sugimoto, M. Fujii, Y. Fukuda, K. Imakita, and K. Akamatsu, *Nanoscale* **6**, 122 (2014).
- ³¹L. Ostrovska, A. Broz, A. Fucikova, T. Belinova, H. Sugimoto, T. Kanno, M. Fujii, J. Valenta, and M. H. Kalbacova, *RSC Adv.* **6**, 63403 (2016).
- ³²H. Sugimoto, M. Fujii, K. Imakita, S. Hayashi, and K. Akamatsu, *J. Phys. Chem. C* **117**, 11850 (2013).
- ³³Y. Hori, S. Kano, H. Sugimoto, K. Imakita, and M. Fujii, *Nano Lett.* **16**, 2615 (2016).

- ³⁴M. Fujii, K. Toshiakiyo, Y. Takase, Y. Yamaguchi, and S. Hayashi, *J. Appl. Phys.* **94**, 1990 (2003).
- ³⁵M. Fujii, Y. Yamaguchi, Y. Takase, K. Ninomiya, and S. Hayashi, *Appl. Phys. Lett.* **85**, 1158 (2004).
- ³⁶M. L. Mastronardi, F. Hennrich, E. J. Henderson, F. Maier-Flaig, C. Blum, J. Reichenbach, U. Lemmer, C. Kübel, D. Wang, M. M. Kappes, and G. A. Ozin, *J. Am. Chem. Soc.* **133**, 11928 (2011).
- ³⁷J. B. Miller, A. R. Van Sickle, R. J. Anthony, D. M. Kroll, U. R. Kortshagen, and E. K. Hobbie, *ACS Nano* **6**, 7389 (2012).
- ³⁸J. Diener, D. Kovalev, H. Heckler, G. Polisski, and F. Koch, *Phys. Rev. B* **63**, 073302 (2001).
- ³⁹P. Roussignol, D. Ricard, C. Flytzanis, and N. Neuroth, *Phys. Rev. Lett.* **62**, 312 (1989).
- ⁴⁰D. J. Norris, M. Nirmal, C. B. Murray, A. Sacra, and M. G. Bawendi, *Z. Phys. D* **26**, 355 (1993).
- ⁴¹M. Nirmal, C. B. Murray, and M. G. Bawendi, *Phys. Rev. B* **50**, 2293 (1994).
- ⁴²M. Nirmal, B. O. Dabbousi, M. G. Bawendi, J. J. Macklin, J. K. Trautman, T. D. Harris, and L. E. Brus, *Nature* **383**, 802 (1996).
- ⁴³M. Bayer, O. Stern, P. Hawrylak, S. Fafard, and A. Forchel, *Nature* **405**, 923 (2000).
- ⁴⁴B. Bruhn, J. Valenta, and J. Linnros, *Nanotechnology* **20**, 505301 (2009).
- ⁴⁵J. Valenta, R. Juhasz, and J. Linnros, *Appl. Phys. Lett.* **80**, 1070 (2002).
- ⁴⁶J. Valenta, A. Fucikova, F. Vácha, F. Adamec, J. Humpolíčková, M. Hof, I. Pelant, K. Kůsová, K. Dohnalová, and J. Linnros, *Adv. Funct. Mater.* **18**, 2666 (2008).
- ⁴⁷I. Sychugov, F. Pevere, J.-W. Luo, A. Zunger, and J. Linnros, *Phys. Rev. B* **93**, 161413 (2016).
- ⁴⁸J. Martin, F. Cichos, and C. Von Borczyskowski, *J. Lumin.* **108**, 347 (2004).
- ⁴⁹J. Martin, F. Cichos, F. Huisken, and C. Von Borczyskowski, *Nano Lett.* **8**, 656 (2008).
- ⁵⁰T. Schmidt, A. I. Chizhik, A. M. Chizhik, K. Potrick, A. J. Meixner, and F. Huisken, *Phys. Rev. B* **86**, 125302 (2012).
- ⁵¹M. D. Mason, G. M. Credo, K. D. Weston, and S. K. Buratto, *Phys. Rev. Lett.* **80**, 5405 (1998).
- ⁵²J. Valenta, R. Juhasz, and J. Linnros, *J. Lumin.* **98**, 15 (2002).
- ⁵³D. S. English, L. E. Pell, Z. Yu, P. F. Barbara, and B. A. Korgel, *Nano Lett.* **2**, 681 (2002).
- ⁵⁴K. Kůsová, I. Pelant, and J. Valenta, *Light Sci. Appl.* **4**, e336 (2015).
- ⁵⁵I. Sychugov, R. Juhasz, J. Valenta, and J. Linnros, *Phys. Rev. Lett.* **94**, 087405 (2005).
- ⁵⁶I. Sychugov, A. Fucikova, F. Pevere, Z. Yang, J. G. C. Veinot, and J. Linnros, *ACS Photonics* **1**, 998 (2014).
- ⁵⁷O. Madelung, *Semiconductors: Group IV Elements and III-V Compounds (Data in Science and Technology)* (Springer-Verlag, Berlin, Heidelberg, 1991).
- ⁵⁸F. Iori, E. Degoli, R. Magri, I. Marri, G. Cantele, D. Ninno, F. Trani, O. Pulci, and S. Ossicini, *Phys. Rev. B* **76**, 085302 (2007).
- ⁵⁹X. Chen, X. Pi, and D. Yang, *J. Phys. Chem. C* **115**, 661 (2011).
- ⁶⁰I. Sychugov, R. Juhasz, J. Valenta, M. Zhang, P. Pirouz, and J. Linnros, *Appl. Surf. Sci.* **252**, 5249 (2006).